LA-UR- 09-04160

Approved for public release; distribution is unlimited.

Title: Large Area Neutron Detector Based on LI6 Ionization Chamber with Integrated Body-Moderator of High Density Polyethylene

Author(s): K. Inakiev
M. Swinhoe
K. Chung
M. Makela

Intended for: Future Meetings and Presentations

Los Alamos
NATIONAL LABORATORY
EST. 1943

Los Alamos National Laboratory, an affirmative action/equal opportunity employer, is operated by the Los Alamos National Security, LLC for the National Nuclear Security Administration of the U.S. Department of Energy under contract DE-AC52-06NA25396. By acceptance of this article, the publisher recognizes that the U.S. Government retains a nonexclusive, royalty-free license to publish or reproduce the published form of this contribution, or to allow others to do so, for U.S. Government purposes. Los Alamos National Laboratory requests that the publisher identify this article as work performed under the auspices of the U.S. Department of Energy. Los Alamos National Laboratory strongly supports academic freedom and a researcher's right to publish; as an institution, however, the Laboratory does not endorse the viewpoint of a publication or guarantee its technical correctness.

Form 836 (7/06)

Abstract/Explanation

These presentation slides and paper are related to the same subject. The presentation slides derive from the paper.

Large Area Neutron Detector Based on ^{6}Li Ionization Chamber with Integrated Body-Moderator of High Density Polyethylene.

K. Ianakiev, M. Swinhoe,

K. Chung, M.Makela

Los Alamos National Laboratory

This work is funded by the US Department of Homeland Security,

Office of Research and Development under contract #HSSCHQ-04-X-00387.

Los Alamos NATIONAL LABORATORY EST 1943

LAUR-05-1032

NNSA

Introduction

- The detector development funded by DHS in 2004 to be a significantly lower cost alternative to ^{3}He detectors
- An 8-cell prototype was built in 2007:
  - Good agreement between simulations and experiment
  - Negligible aging for a 6 month period
- Work terminated because the manufacturing cost was greater than originally estimated. Now, cost is not the primary criterion.
- We have an improved path forward with a method for mass production.

Detection Concept

- ^{6}Li foil lined ionization chamber with fill gas at one atmosphere and pulse mode operation.
- High-density polyethylene (HDPE) body serves also as a neutron moderator.
- Tolerant to HDPE outgassing products by principle of operation.
- All electrodes, including high voltage bias supply are hermetically sealed within the plastic slabs.
- The ^{6}Li foil serves also as a getter for gas poisons O_2, CO_2, and H_20 vapors.

Design concept of cell with parallel plate anode

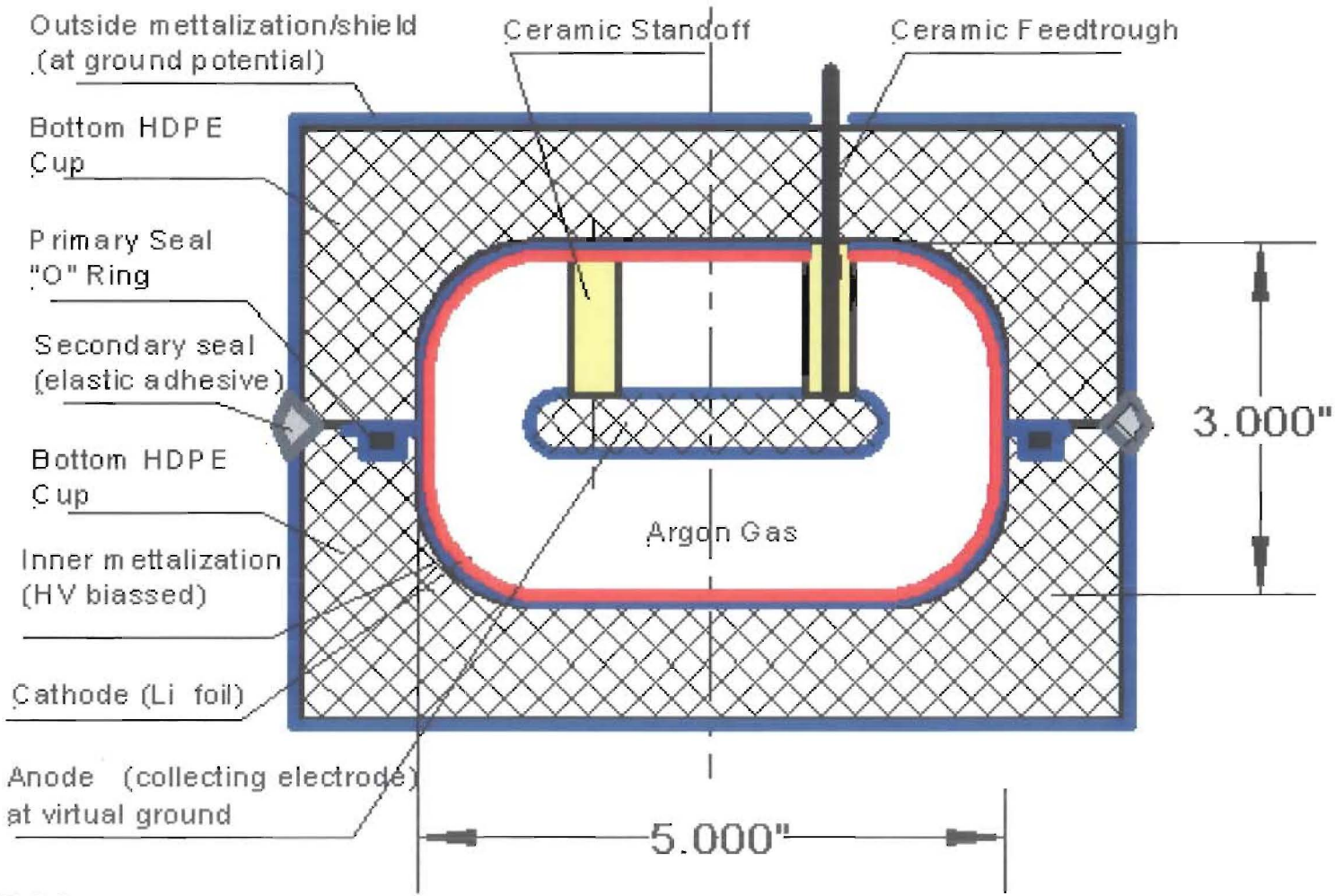

Intrinsic efficiency of ^{6}Li foil for omni-directional thermal neutron flux

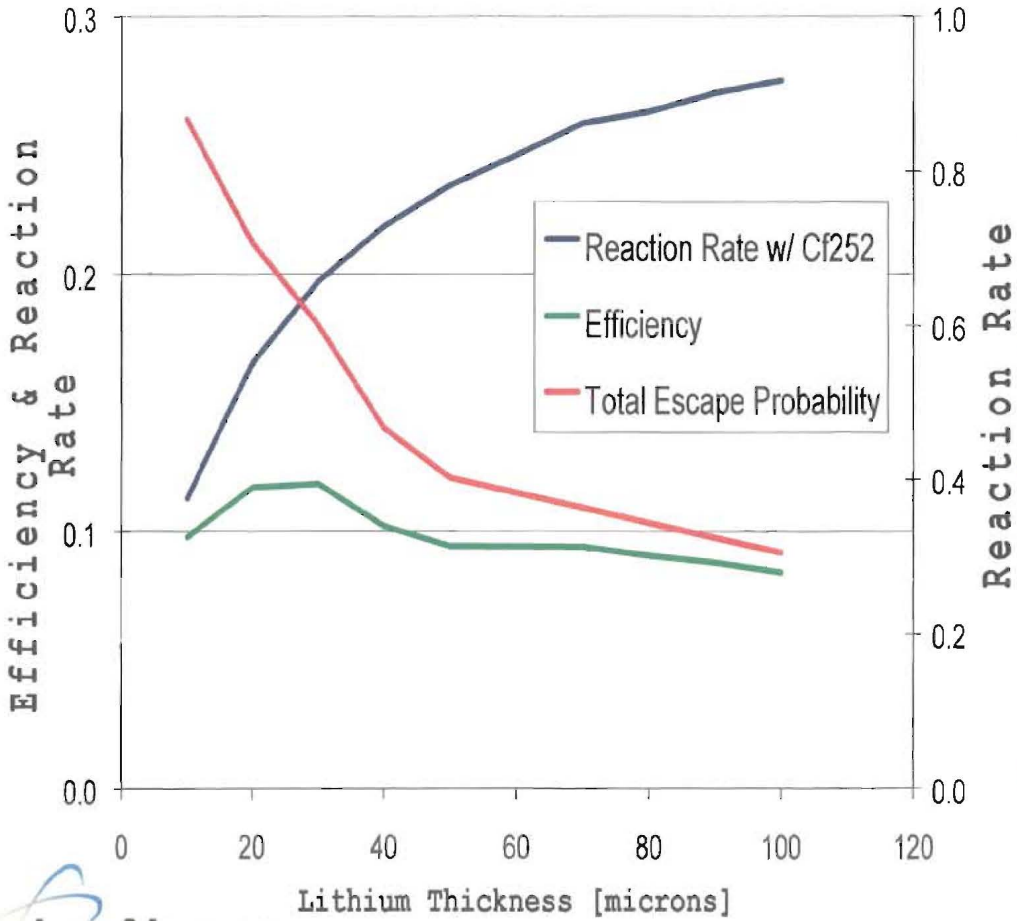

- The $^{6}Li(n,\alpha t)$ reaction rate increases with thickness (Monte Carlo calculation)
- The fraction of tritons and alphas that escape decreased with increasing thickness (analytically calculated)
- The detection efficiency is the product of these factors
- The maximum efficiency is obtained for lithium foils with thickness in the range 20 -30 microns. The tritons provide 76% and alpha particles 24% of total signal
- Calculations agree within 10% for single-cell prototypes

Los Alamos NATIONAL LABORATORY EST 1943

Choice of working gas mixture

Our preference is for Argon-Methane gas mixture:

- Reasonable electron velocity can be achieved at lower field strength, giving lower microphonic sensitivity.
- The flammability concentration for the methane is 9% versus 2% for the isobutane.
- HDPE outgas products act as gas admix
- Optimized electrical field configuration: Change of gas admix from 2% to 14% causes only 20% variations in electrons drift velocity

Calculated electron drift velocity in argon-methane gas mixture

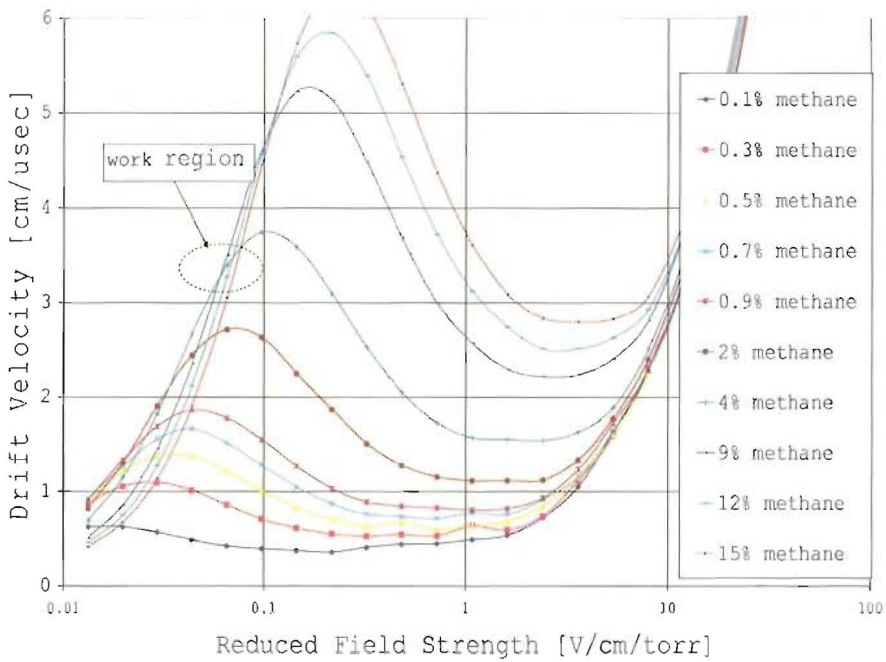

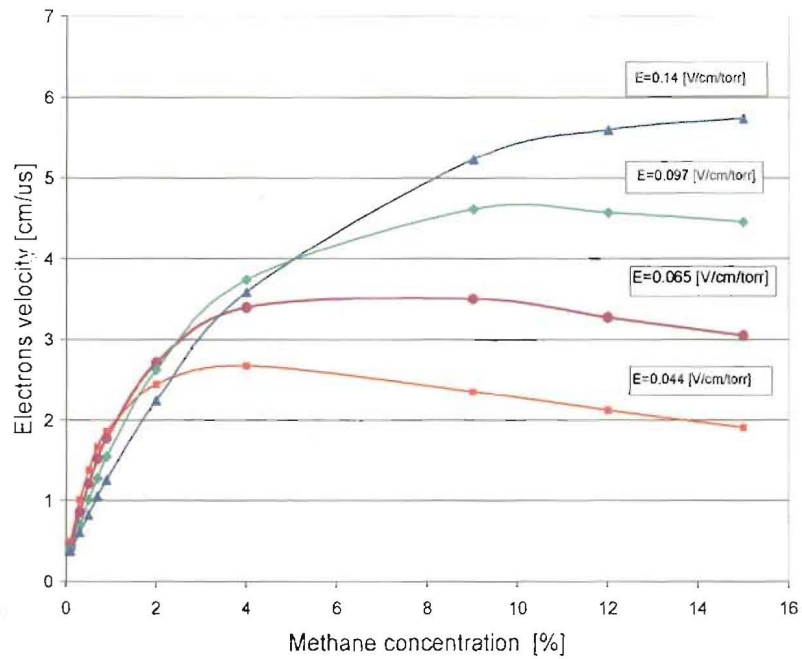

The electron drift velocity is not sensitive to the methane concentration between 3% and 15% at a reduced field strength of 0.07 V/cm/torr

Neutron (Cf-252) and Gamma (Cs-137) Pulse Height Spectra

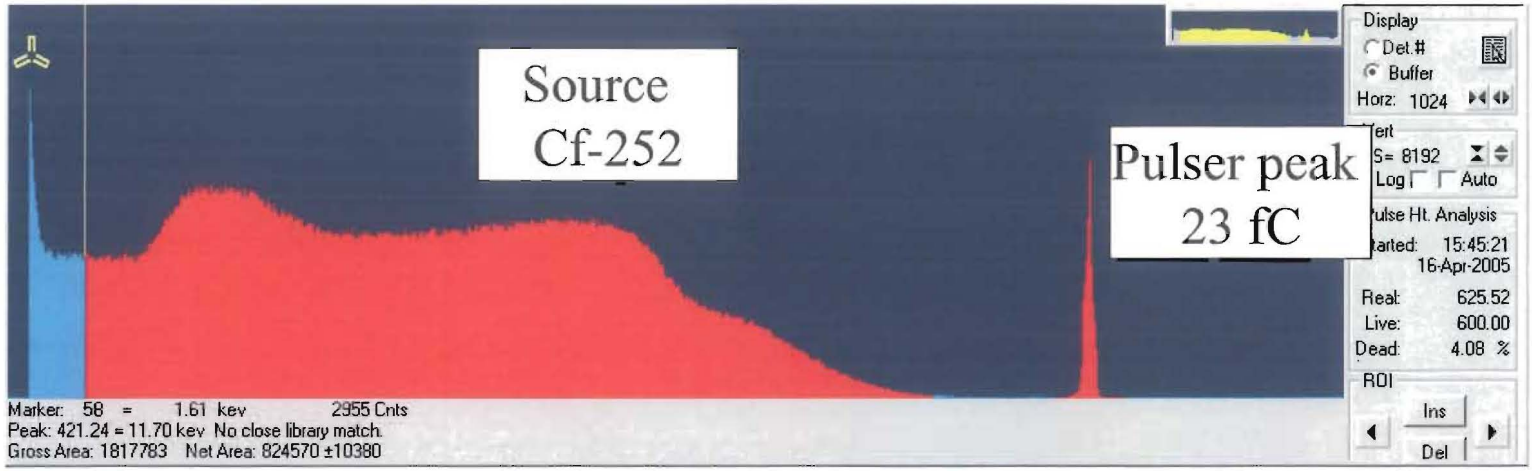

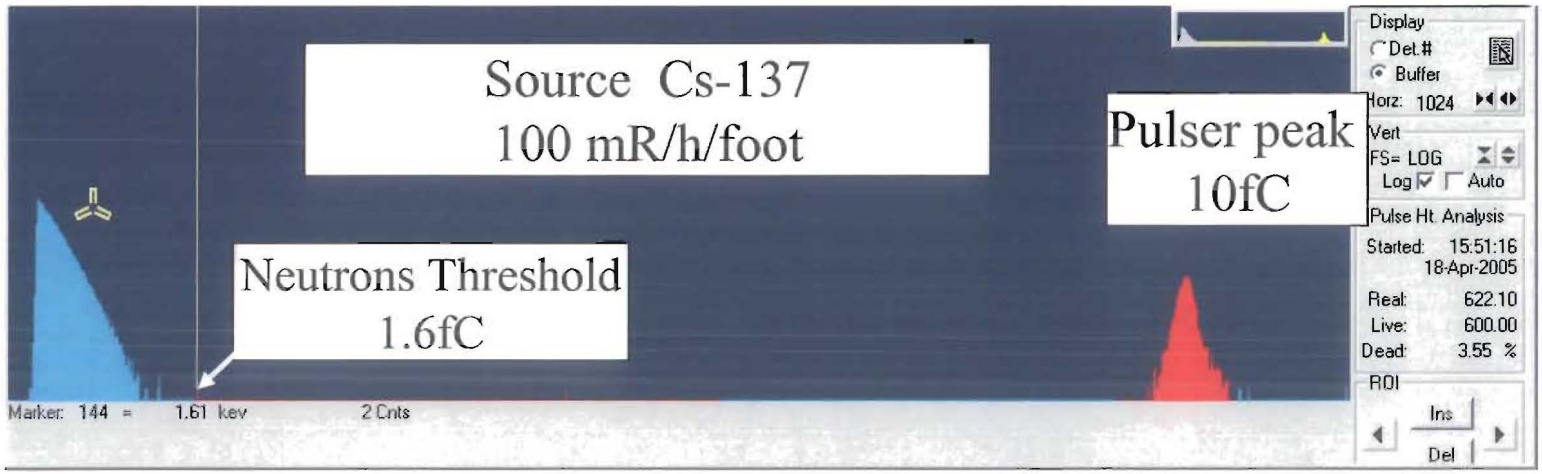

Efficiency optimization in 2 by 9 cell array of 5"by 5" by 3"square shape cells

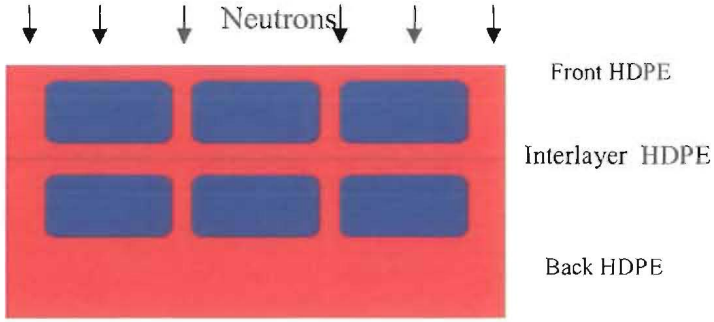

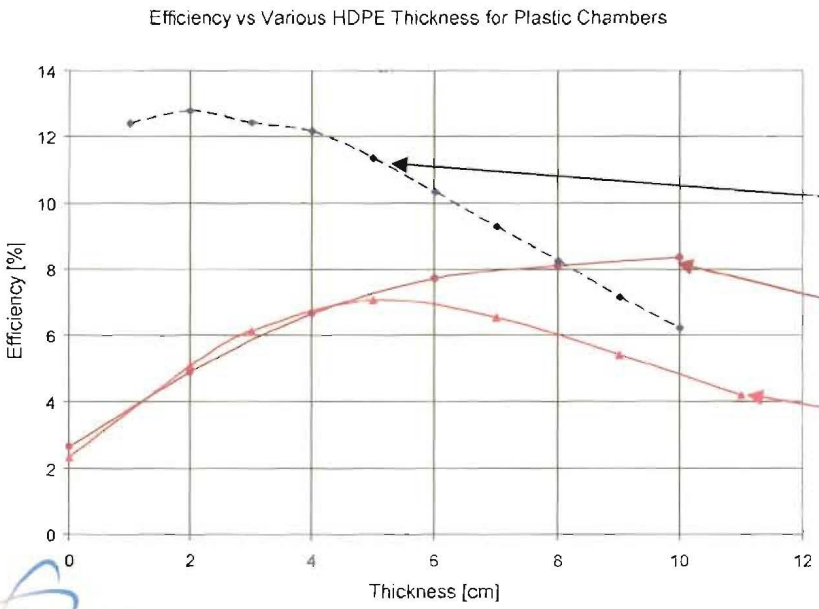

- The detection efficiency was calculated for a 3 × 3 × 2 array of square cells with size 5"by5"by3"embedded in HDPE
- The ^{252}Cf neutrons were incident in a parallel beam
- The efficiency was calculated:

  as a function of front thickness with optimized rear thickness
  - as a function of front thickness with optimized interlayer and rear thickness
  - as a function of rear HDPE thickness
  - as a function of front thickness (back and int. thickness 1cm)
- Maximum efficiency = 13%

Los Alamos NATIONAL LABORATORY EST 1943

8 Cell ^{6}Li Detector – Fabrication Process

8 Cell ^{6}Li Detector – Prototype Assembly

Los Alamos NATIONAL LABORATORY EST 1943

Efficiency Measurements

Measurement	Measurement condition	Reaction Rate [/sec] (MCNPX)	Relative Error [%]	MCNPX Pulse Counts (90% ROI)	Measured pulses (background subtracted)	Difference [%]
1	Center of Side B, on the surface	0.072206	0.0006	22597941.2	22734459	-0.60
2	Center of Side B, 10 cm from surface	0.035765	0.0008	11193156.2	12506548	-10.50
3	Center of Side B, 50 cm from surface	0.004712	0.0023	1474809.3	1643931	-10.29
4	Center of Side B, 100 cm from surface	0.001365	0.0042	427278.1	539298	-20.77

Effect of Six-Month Aging - Comparison of Pulse-Height-Spectra.

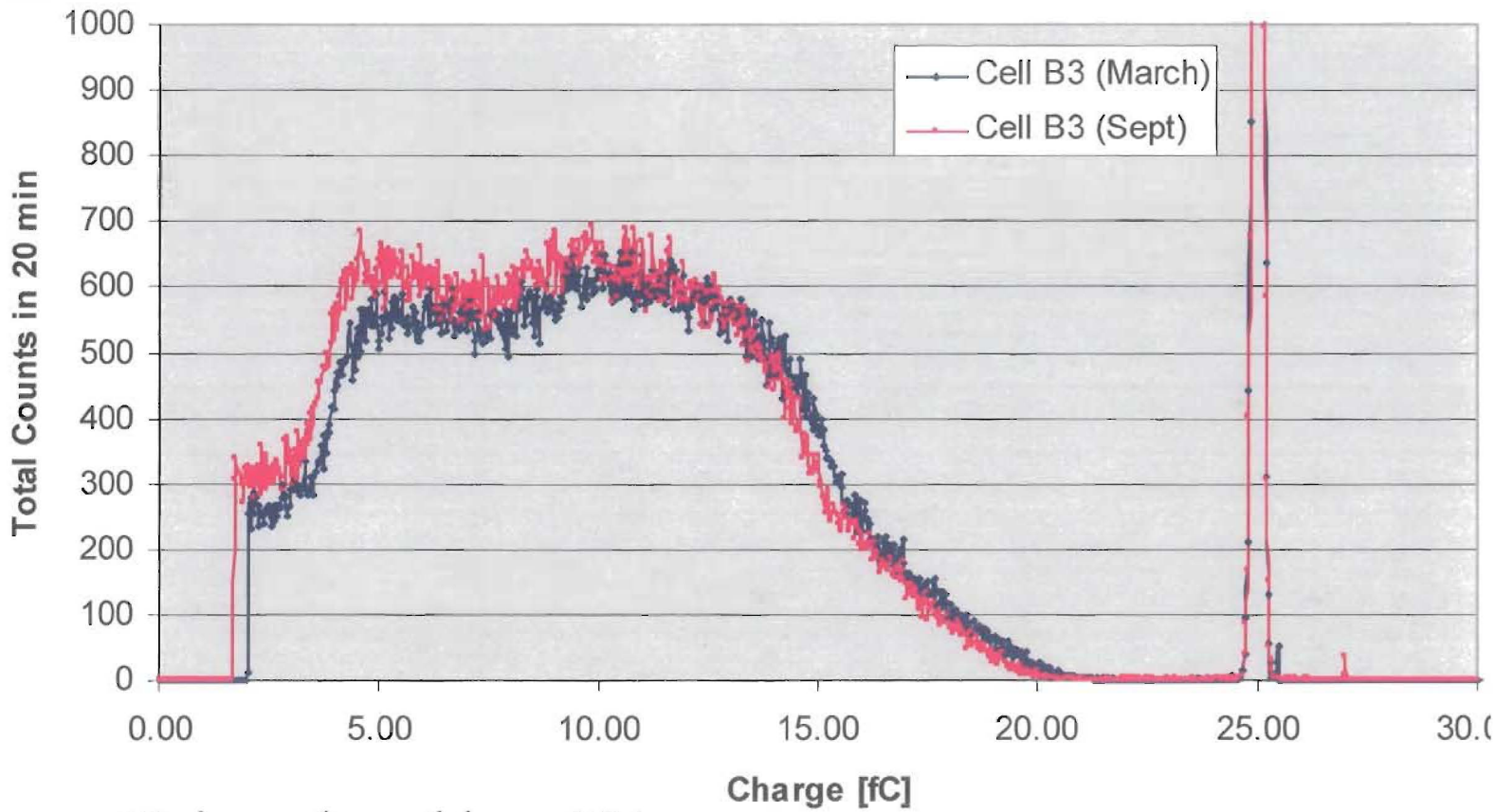

- Gain reduced by ~2%
- Count rate unaffected because of integral counting mode

Los Alamos NATIONAL LABORATORY EST. 1943

Conclusions

- A proof of principle prototype shows good agreement between simulations and experiment
  - **About 13% intrinsic efficiency for fast neutrons**
  - **Negligible aging for 6 months**
- At similar cost per unit efficiency this technology could be a alternative replacement of ^{3}He detectors.
- We have an improved path forward with a method for cost-effective mass production.

LARGE AREA NEUTRON DETECTOR BASED ON LI6 IONIZATION CHAMBER WITH INTEGRATED BODY MODERATOR OF HDPE

8-cells Prototype Experimental Results

I. Introduction

The fabrication and testing of a prototype detector array (figure 1) posed significantly more issues than single-cell prototype detectors due to the size of polyethylene blocks and the complexity of the inner volume of the detector array. The 8-fold increase in the inner surface area and interface increases the overall outgas rate and possibility of microscopic leaks occurring at the interface, risking the long-term fill-gas integrity. While the increased outgas rate may be small, the accumulated and combined effect may shorten detector's continuous operation, requiring more frequent servicing and longer service time for the detectors.

Figure 1. Machined, bare polyethylene body; 2 lids and 1 middle piece (center).

The purposes of this series of experiments with the prototype detector array are:

To ensure there is no leak,
To ensure the overall outgas rate is within the operational parameter,
To obtain stability of performance for each cell, and
To compare the experiment results with MCNPX simulation.

II. Testing of Seal Integrity

After polyethylene pieces were machined, as shown in Figure 1, and their surfaces were metallized (Figure 2), different types of gaskets were used to test the seal of the interface. The total length of seal interface for the polyethylene bodies is approximately 220 cm and the use of components off the shelf (COTS) viton gasket or silicone sheet gaskets resulted in measurable leaks. In the end, custom-made viton o-rings of 55 durometer, 0.53 cm of cross section, and 109.47 cm of developed length prior to the formulating, were used. The dimensions of the perimeter groove are 6.1 mm wide and 3.8 mm deep. The o-ring would fill the groove approximately 90% at full compression and would allow small movement in the channel to minimize rubbing, which is necessary to ensure the longevity of the o-ring. The center o-ring was fabricated out of a silicone sheet of similar hardness of 60 durometer. The use of customized silicone o-ring was necessary because the small radius of curvature for the center groove would not allow gluing of viton material into an o-ring.

Figure 2. Polyethylene body with 4-micro thick nickel and stainless steel metallization.

The o-rings were then lubricated with Dow-Corning High Vacuum Grease, and the polyethylene bodies were assembled together with bolts using a torque wrench set at 10 lbf-in. 17 bolts were tightened with a torque wrench in a diagonal order to ensure uniform distribution of pressure across the polyethylene bodies. Using a Pfeiffer Vacuums QualyTest Dry HLT 270 leak detector, the detector array was tested for vacuum integrity. The leak detector can detect trace amount of helium with an accuracy of 10^{-10} mbar*liter/sec of flow rate, which was more than adequate for detecting leak rates of the detector array. Using a helium spray probe, seal integrity was checked and the entire

interface was confirmed to be vacuum tight. The background flow rate of helium was recorded as 1.6×10^{-8} mBar*liter/sec, which became the practical limit of detection for the experiment conditions. The leak tests were performed on all sides, including valves and signal wire connections, and showed there is no detectable penetration of helium atoms.

This is a significant step in proving the structural integrity of the seal and of the body as maintaining gas purity within the design specification is a crucial factor in deciding the lifespan of the detector. Even though helium will not be used in fill-gas and the detector will not operate in vacuum, the leak tests were performed with helium in vacuum condition because of the helium atoms' small size, low background concentration, ready availability and their inertness to react with surrounding atoms. For example, the atomic radius of a helium atom is 31 picometer, whereas an argon atom's is 71 picometer, effectively giving a helium atom less than a quarter cross section than that of an argon atom. The diffusion coefficients of helium, argon and methane in polyethylene are 57E-7, 4.5E-7, and 1.9E-7 cm^2/sec, respectively (Flaconneche et al, 2001). The difference in diffusion coefficients shows that the helium atoms are more than 10 times more mobile than argon atoms in polyethylene. This conservative test will emphasize the robustness of the seal of the detector and thereby assure the longevity of the detector operation.

Figure 3. Close-up of o-ring placement

The long-term leak tests saturating the entire detector array in a helium medium were not performed because the mobility and size of the helium atoms would allow penetration

eventually through the polyethylene body. The leakage through structural failures at the seal interface would readily show up with short-term helium leak tests. Permeability rate would be analogous to longer-term leak tests because permeation may be considered a long-term, three-stage process that includes absorption, diffusion and desorption (Gerlach et al, 2001). The helium permeability rates through polyethylene and viton are comparable at 2E-7 and 1.2E-7 cc/sec/cm^2/cm at 1 atmospheric pressure at 25 Celsius (1cc of helium per second per cm^2 of surface area per cm of thickness at 1 atm), respectively. The permeability rate through silicone is 23.8E-7 cc/sec/cm^2/cm at 1 atmospheric pressure at 25 Celsius (Varian Associates, 1980). A comparison study of permeability rate showed argon atoms, the main constituent in the fill-gas, at 0.76E-7 cc/sec/cm^2/cm at 1 atmospheric pressure at 61 Celsius, while the same study showed 2.1E-7 cc/sec/cm^2/cm at 1 atmospheric pressure at 59 Celsius (Flaconneche et al, 2001). The permeability rate of methane, which is the other constituent in the fill-gas, was observed at 1.2E-7 cc/sec/cm^2/cm at 1 atmospheric pressure at 60 Celsius (Flaconneche et al, 2001).

III. Outgas Rate and Composition

One of the novel design aspects of the detector array is the use of polyethylene bodies as an integral part of the detector. Conventional gaseous thermal neutron detector designs would have a clear separation of moderating part and active volume of gas detector where thermalized neutrons interact with fill-gas atoms. However, in this detector design, the separation of energy-moderating volume and the active volume of the detector where charge collection occurs is established by 4-micron thick metallization layer. The advantage of this design is that the use of an integral polyethylene body allows employing widely available manufacturing methods to mass-produce inexpensively the polymer bodies. Unfortunately, it also brings on contamination of fill-gas by outgas from the body. The outgas can cripple the detector operation, even with detector being air-tight, by altering the fill-gas composition from within and by disrupting the processes in creating secondary electrons, which are the main signal carriers (Knoll, 2001). Therefore, ascertaining the outgas composition and rate to establish a window of tolerance are fundamental in designing operational specification.

The outgas rate measurements were performed under vacuum to utilize pressure gradient; without the use of vacuum, it would have been prohibitively long experiments to collect measurable amount of outgas. The inside dimensions of the outgas chamber, which was a section of a cylindrical pipe ended with two metallized polyethylene pieces, were measured as 9.73 cm of inner diameter and 10.16 cm of height. The total surface area of outgas was calculated as 270.91 cm^2 and the volume of the chamber was calculated as 755.18 cm^3. This chamber was pumped with a turbo vacuum pump attached to a residual gas analyzer (Stanford Research Systems, RGA-100). The chamber was pumped out to 10^{-8} torr of vacuum and the inside pressure was recorded with a mensor gauge to obtain the outgas pressure accumulation. During 238 days of monitoring, there was 3.9 torr of accumulation

inside (Ianakiev, 2004). This overall outgas rate of 9.6E-10 torr-liter/(cm^2-sec) was approximately 2 orders of magnitude better than published outgas rate data (of the bare polyethylene. When the overall outgas rate also took into consideration from the cylinder wall which was made out of stainless steel, then the outgas rate drops further to 5.3E-10 torr-liter/(cm^2-sec). This reduced rate clearly shows outgas of the polyethylene is prevented by certain mechanism.

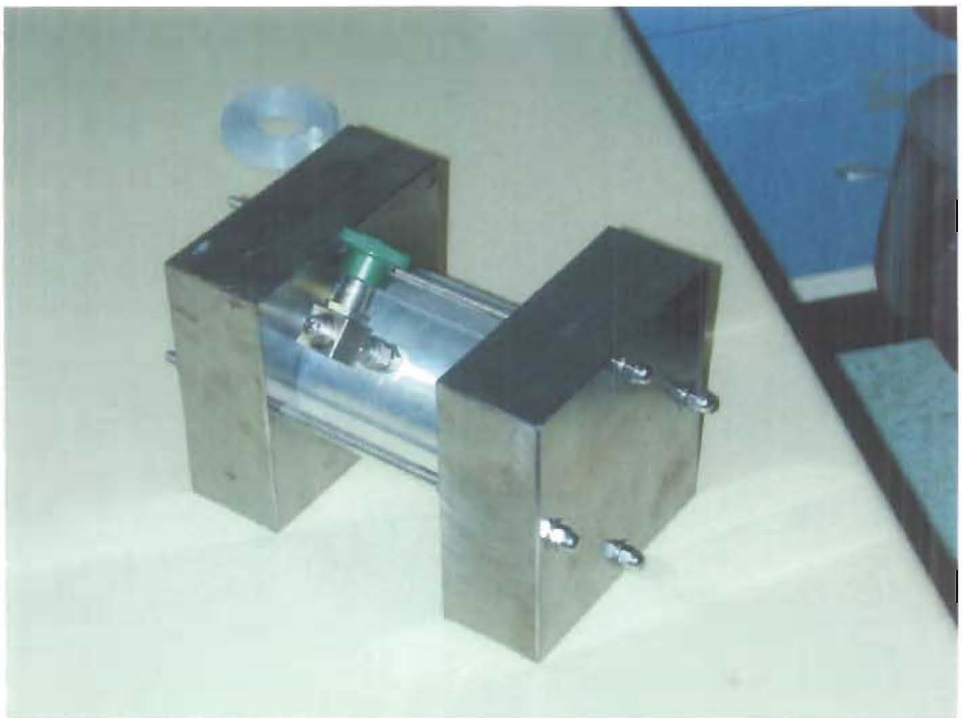

Figure 4. A cylindrical chamber with HDPE ends used to obtain outgas data.

A partial explanation of the reduced outgas rate can be attributed to the metallization layer. The 4-micron thick metal film may act as an atomic barrier and hinder the migration of outgas from the polymer lattice to the vapor phase, thereby reducing the outgas. Unfortunately, this explanation cannot fully explain the 2 orders of magnitude reduction in the outgas. It is conceivable that the metallization aided in reducing the flow of outgas, but a bulk of credit can be given to the partial pressure inside the polymer matching the partial vapor pressure in the vacuum to impede the diffusion of the outgas components (Segovia, 1999). Overall, the final, stable outgas rate of 0.3 torr/month has been shown to be tolerable for approximately 20 years of continuous operation when electron dynamics was simulated using Garfield (Chung et al, 2005).

With the overall outgas rate quantified, the components of the outgas were identified using two different methods. The first method was performed using a residual gas analyzer (RGA). The advantages of this method is that the setup of the system is rather compact and simple so that analyses can be performed on site, next to the outgas chamber, with minimal

calibration. There is no need to take a sample and send it off to an off-site laboratory for results. The analyses using a Stanford Research Systems RGA-100 indicated the outgas was mostly made up of environmental components such as water (43.92%), carbon dioxide (6.239%), nitrogen (39.37%), argon (1.081%), and oxygen (9.389%).

IV. Baseline Measurement

Having quantified the outgas rate and composition, a series of initial measurements have been performed to establish the performance of individual detector cells, prior to obtaining the detector matrix performance as a whole. Because the 95% enriched lithium-6 used in the detector matrix is highly reactive with moisture in the air and was assembled by hand in a dry room in a lithium battery fabrication facility, the material will not be readily repaired at LANL without the use of such a facility. Since there was little chance that the chambers will be repaired at LANL, there was a need to establish a baseline measurement for each cells so that the individual performance over the period can be compared. Side B of the detector array was prepared first with detector electronics and was available for the baseline measurement. Figure 5 shows a can of 95% enriched lithium-6 foil that was manufactured in 2003. The can was sealed with argon gas, and was in storage for three years.

Figure 5. Ninety-five percent enriched lithium-6 metallization material.

Figure 6 shows the interior surface of the detector matrix after lithium foil was manually laid out. The difference in the gleam of the surface when compared to Figure 3 is not due to difference in lighting. Figure 7 is the close up of the surface and patchwork of small strips of lithium-6 foil can be seen. After lithium-6 foil lamination work was finished, the detector array was assembled in the dry room, and prepared for shipping to LANL. The exterior of the detector array was visually inspected upon arrival and was retested with helium leak detector for seal integrity. The detector array passed the test and was prepared with electronics for initial measurements.

Figure 6. Lithium metallization is applied on the interior surface.

Figure 7. Close-up of the lithium metallization.

Figure 8. Fully assembled detector array with detector electronics.

The baseline measurements were conducted in March 2007, when the detector array arrived at LANL. First, the individual gain of the electronic boards and detector cells has been equalized using a potentiometer on the boards. Having verified that the individual detectors have the same gain, initial measurements began. An electronic pulser peak was established at 25 fCoulomb as an indicator of electronic noise level. A Cf-252 source was placed at the center of detector cells for 20 minutes and the spectra were recorded. Figure 9 indicated that the there is some minor change in the charge collection efficiency between the spectra taken in March and September of 2007 (redistribution from high energy region to low energy region in the spectrum). Because of gross counting, this change should not affect the counting characteristics because wast majority of the spectrum is still above the threshold. The Further neutron efficiency measurement described in V will be need to assess the effect of aging progress.

Figure 9. Six-month Comparison of Cell B1 Spectra.

Figure 10. Six-month Comparison of Cell B2 Spectra.

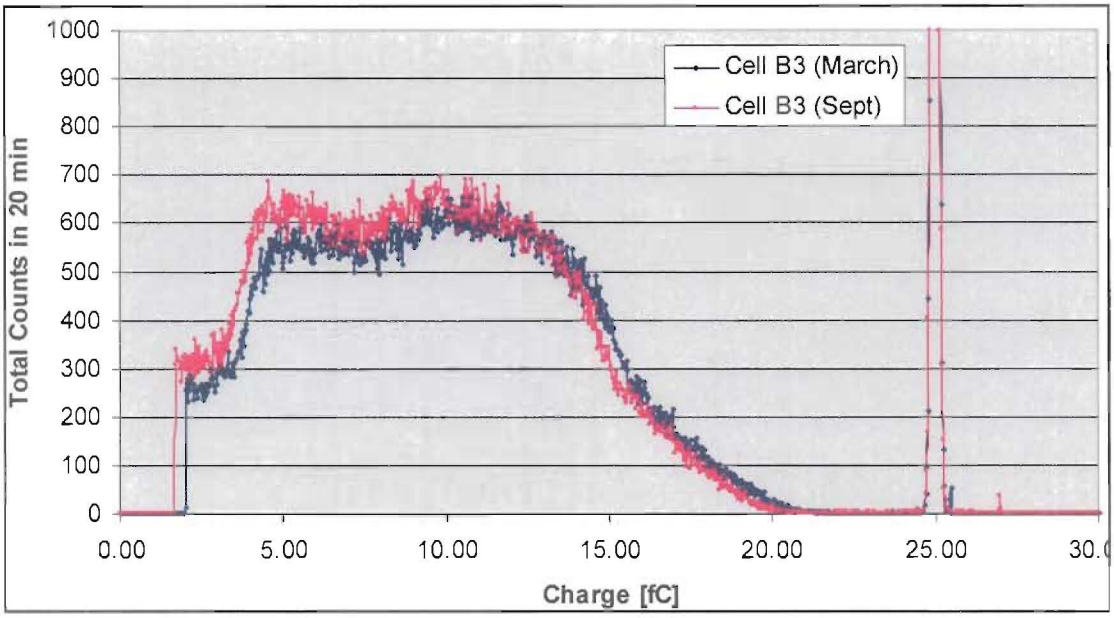

Figure 11. Six-month Comparison of Cell B3 Spectra.

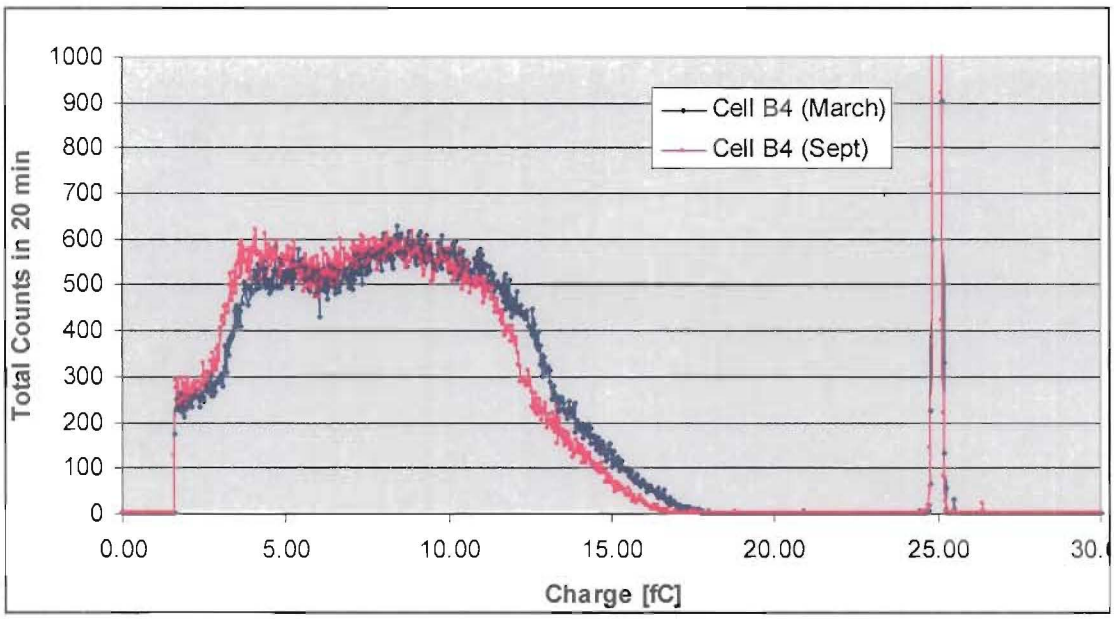

Figure 12. Six-month Comparison of Cell B4 Spectra.

V. Comparison of Detector Array Measurement and MCNPX Simulations.

For measurements 1 through 4, the same Cf-252 source was placed at the center of cell B1, B2, B3, and B4. In the MCNPX simulation, a point source was placed at the center of individual cells. The measurements 1 through 4 indicated close agreement with their respective simulation counterparts. The Cf-252 source was placed at the center of the side B for measurement 5 and for measurement 6 through 8, the source was moved out from the center of side B by 10 cm, 50 cm, and 100 cm, respectively. As the distance between the source and the detector array became longer, the difference between the simulation results and measurement became more apparent, notably with measurement 8 whose difference was approximately 21%.

Table 2. Comparison of MCNPX simulation and experimental results.

Measurement	Measurement condition	Reaction Rate [/sec] (MCNPX)	Relative Error [%]	MCNPX Pulse Counts (90% ROI)	Measured pulses (background subtracted)	Difference [%]
1	Center of B1	0.081513	0.0005	25510684.1	23922817	6.63
2	Center of B2	0.072087	0.0006	22560657.9	22378119	0.81
3	Center of B3	0.072124	0.0006	22572131.2	23654360	-4.34
4	Center of B4	0.072189	0.0006	22592473.8	23757490	-4.90
5	Center of Side B, on the surface	0.072206	0.0006	22597941.2	22734459	-0.60
6	Center of Side B, 10 cm from surface	0.035765	0.0008	11193156.2	12506548	-10.50
7	Center of Side B, 50 cm from surface	0.004712	0.0023	1474809.3	1643931	-10.29
8	Center of Side B, 100 cm from surface	0.001365	0.0042	427278.1	539298	-20.77

VI. Conclusion

The detector array, which posed more complex problems from machining to ensuring seal integrity was put through machining, metallzation, leak test, and lithium-6 lamination. In the process, the outgas volume and component analyses were performed to ensure continuous operation would be viable. It has been determined that the detector array can operate continuously with the outgas volume and the composition.

Overall, the verification of MCNPX calculation has been positive, showing close agreement in most of the measurements.

VII. References

B. Flaconneche et al, Oil & Gas Science and Technology. 56 (2001) 3 261.

A. Berlach et al, Microsystem Technologies 7 (2001) 17.

Varian Associates, Inc. Introduction to Helium Mass Spectrometer Leak Detection, 1980.

K. Chung et al. Mitigation of Outgas Effects in the Neutron-Capture Li^6 Pulse-mode Ionization Chamber Operation. presented at 2005 IEEE Nuclear Science Symposium

G. Knoll, Radiation Detection and Measurement. 2000.

K. Ianakiev et al, Large Area Neutron Detector Based on ^{6}Li Ionization Chamber with Integrated Body-Moderator of High Density Polyethylene. Presented at 2004 IEEE Nuclear science Symposium.

J.Hendricks and G.McKinney, MCNPX v2.5, Los Alamos National Lab, 2007.

J. de Segovia, CERN Accelerator School Vacuum Technology, 28 May, 1999, pg 99.

Mid-year Review of RD Program Office Investments
May 11th 2009

New material technology for thermal neutron detection using Li containing semiconductors.

Project Goal : Obtain data and submit full NA-22 proposal

Project Budget: total $100k ; spent ~$75k

Project Team: K. Ianakiev, J. C. Lashley, J. L. Smith, B. Mihalia, R. Muenchausen, and M. Swinhoe LANL, P. B. Littlewood University of Cambridge

Photoconductivity experiment – cryostat assembly

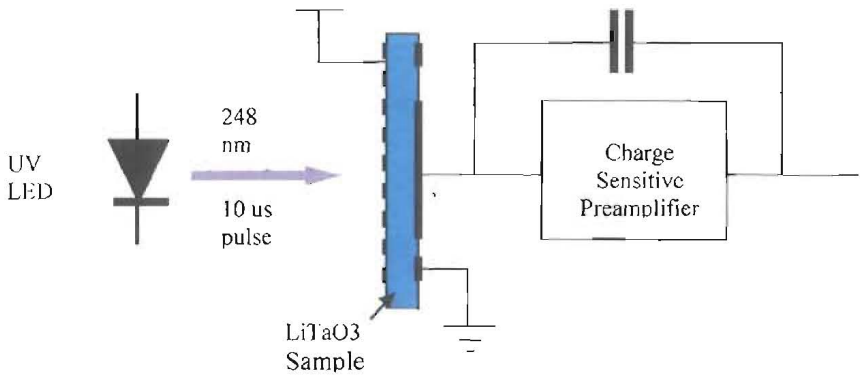

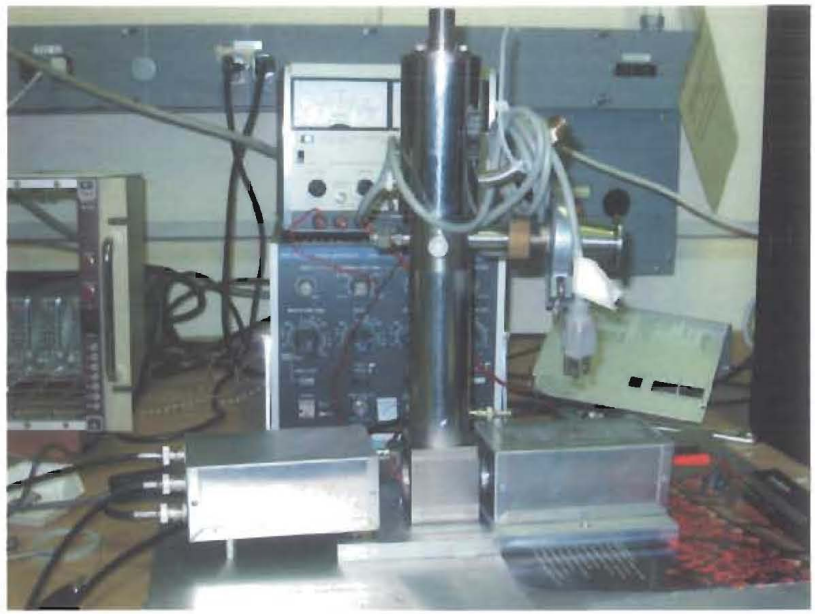

- Improved sensitivity ~ 5V/pC
- Improved noise ~ 1.6 nV/hZ^0.5
- Capability for work from cryogenic to 150C

Photoconductivity experiment – Incident photons calibration

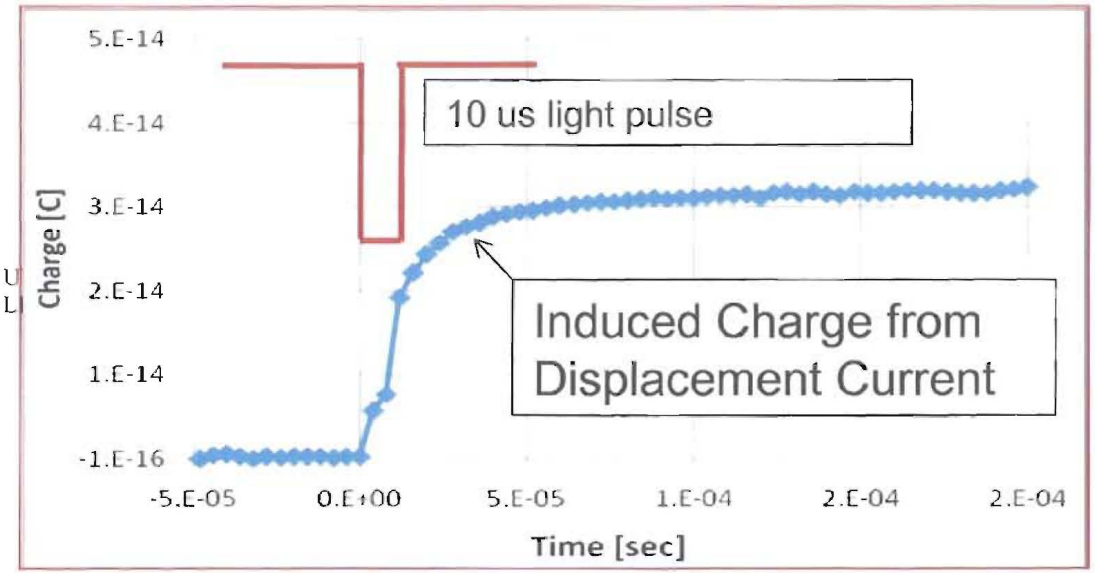

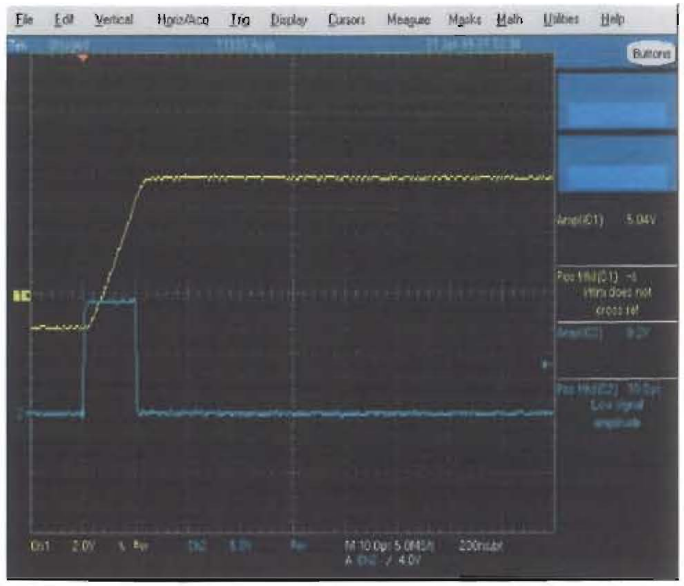

- Use 100% UV QE Si detector IRD
- Incident numbers of photons 2.1E8
- Measured charge 30 fC => 2E5 photons
- Estimated average carriers displacement ~ 200nm KI1

Slide 3

KI1 Clear this with Peter.
120030, 5/8/2009

Build Strong Collaboration with Universities and Academia

Los Alamos National Laboratory- Photoconductivity and radiation measurements

K. Ianakiev, J. C. Lashley, J. L. Smith, B. Mihalia, R. Muenchausen, and M. Swinhoe

Boston College Material modification

C. P. Opeil

University of Cambridge Charge transport modeling

P. B. Littlewood

Sandia National Laboratory – Contacts design and traps study

A. Armstrong and R. M. Fleming

Joint LANL- SNL Proposal for one Year Feasibility Study Submitted

- *Proposal Title*:
Thermal Neutron Detection Technology Based on Single Crystal Lithium Tantalate ($LiTaO_3$).

- *Funding*:
LANL 600k, SNAL 600k

- *Proposal status*:
Passed internal NA-22 review, sent to external reviewers

Future work

Use the rest of funding to leverage chances for this and future projects:

- Submit a paper for upcoming NSS meeting.
- Can we support Boston College for material modification capabilities?
- Develop small area thin sample for demonstration of radiation response for inclusion in FY11 full proposal

LiNbO3 Data from FEJER Group web page

Many properties depend on stoichiometry

- Congruent crystals have large density of point defects
  - ~1.5% Li deficient

$$x \equiv \frac{[\mathrm{Li}]}{[\mathrm{Li}]+[\mathrm{Nb}]}$$

- Carrier lifetime: $\tau \propto \frac{1}{N_{traps}} \propto \frac{1}{(0.5-x)+\mathrm{ppm}}$
- Conductivity: $\sigma \propto \mu\tau \propto \frac{1}{N_{traps}} \propto \frac{1}{(0.5-x)+\mathrm{ppm}}$
- Ferroelectric coercive field [Gopalan 2000]

$$E_c \propto 0.5 - x$$

- 20000 V/mm congruent
- 100 V/mm stoichiometric LT

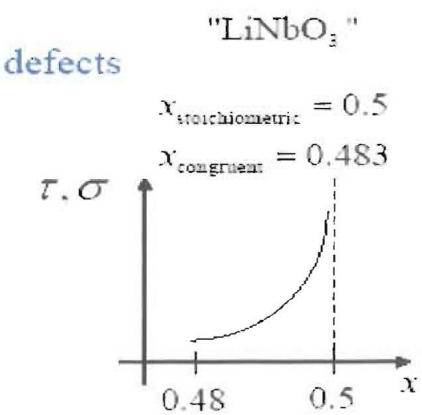

most of change for final ~0.01 in x